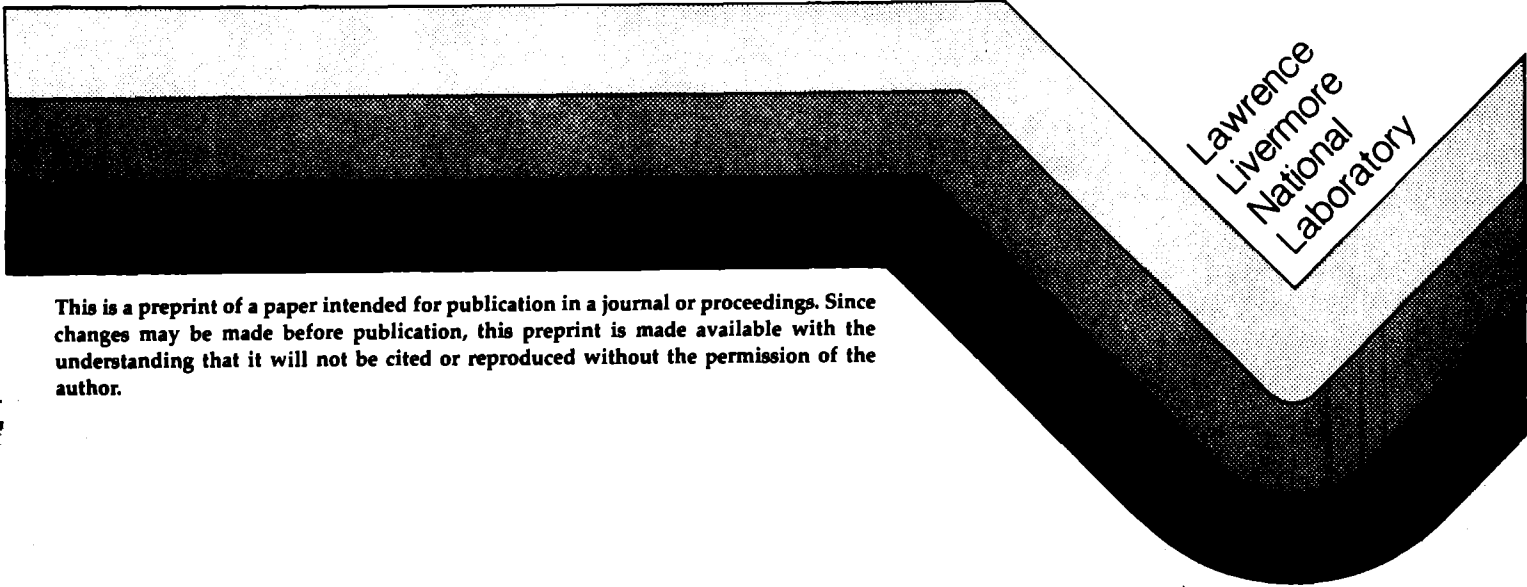Plasma Heating and Current Drive
Using Intense, Pulsed Microwaves

B. I. Cohen
R. H. Cohen
W. M. Nevins
T. D. Rognlien
P. T. Bonoli
M. Porkolab

This paper was presented
at the Joint Varenna-Lausanne
International Workshop on
"Theory of Fusion Plasmas"
Chexbres, Switzerland

October 3-7, 1988

Lawrence
Livermore
National
Laboratory

DISCLAIMER

PLASMA HEATING AND CURRENT DRIVE USING INTENSE, PULSED MICROWAVES

B.I. Cohen, R.H. Cohen, W.M. Nevins, and T.D. Rognlien
Lawrence Livermore National Laboratory,
University of California
Livermore, CA 94550 USA

P.T. Bonoli and M. Porkolab
Massachusetts Institute of Technology
Cambridge, MA 02139 USA

The use of powerful new microwave sources, e.g. free-electron lasers and relativistic gyrotrons, provide unique opportunities for novel heating and current-drive schemes in the electron-cyclotron and lower-hybrid ranges of frequencies. These high-power, pulsed sources have a number of technical advantages over conventional, lower-intensity sources; and their use can lead to improved current-drive efficiencies and better penetration into a reactor-grade plasma in specific cases. The Microwave Tokamak Experiment at Lawrence Livermore National Laboratory will provide a test for some of these new heating and current-drive schemes. This paper reports theoretical progress both in modeling absorption and current drive for intense pulses and in analyzing some of the possible complications that may arise, e.g. parametric instabilities and nonlinear self-focusing.

I. Introduction

This theoretical study addresses the physics of intense microwave heating and current drive in toroidal systems. High-power microwave sources have been successfully used to heat and drive current in tokamak plasmas in both the electron-cyclotron and lower-hybrid ranges of frequency. Electron-cyclotron heating (ECH) has been effective in heating plasmas, driving current, and inducing the transition to improved confinement (H-mode), and it has the technical advantage of allowing remote launching of the waves with simple structures of relatively small size. Lower-hybrid waves have been quite effectively used to heat plasmas and drive current. The launching structures (waveguide arrays and grills) and coupling to the plasma are somewhat more complicated for lower-hybrid heating.

Several concepts exploiting new high-power microwave sources are described and analyzed here. We first consider the application of free-electron lasers (FEL's) as envisioned in the Microwave Tokamak Experiment (MTX)[1] at Lawrence Livermore National Laboratory in cooperation with the Massachusetts Institute of Technology to electron-cyclotron heating (Sec. II) and current drive (Sec. III). Three novel schemes are described that exploit FEL technology to produce current drive at high efficiencies. The new concept of using pulsed, high-power lower-hybrid waves to better penetrate a hot plasma is discussed in Sec. IV. A number of complications (e.g., parametric instabilities and nonlinear self-focusing) that can arise in applying very intense waves to heat plasma and drive current are considered in Sec. V. The importance of these complications influences whether the intense microwaves can be successfully used for the intended applications. Some concluding remarks are presented in Sec. VI.

II. Intense ECH with Free-Electron Lasers

The use of short-pulse, high-power FEL's as microwave sources affords several opportunities for novel new electron-cyclotron heating and current-drive schemes, and possesses a number of technological advantages, e.g., frequency tunability, quasi-optical beam transport, windowless transmission, and reduced possiblity of dielectric breakdown. MTX will provide the first tests of the applications of a high-power FEL to ECH in a tokamak.[1]

Because of the high power (P = 3-8GW) delivered in short pulses ($\tau_{\text{FEL}} \leq 50$ ns) in MTX, the wave electric field will be quite large ($E_0 \sim 500$ kV/cm). Consider electrons that satsify the relativistic cyclotron resonance condition

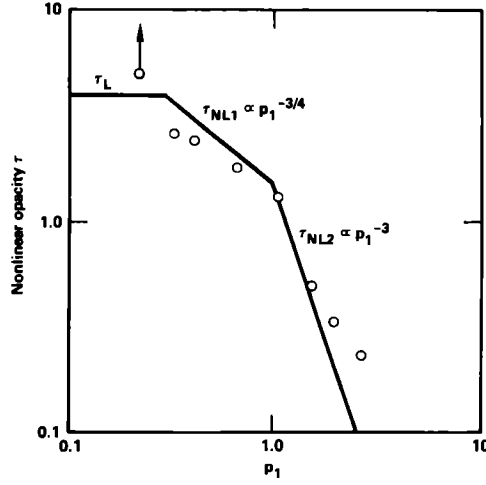$$\omega - \ell\Omega_0/\gamma - k_\| v_\| = 0, \tag{1}$$

Figure 1: Nonlinear opacity $\tau \equiv -\ln$ (transmission coefficient) vs. p_1 for O-mode heating at perpendicular incidence from ZOHAR simulations.

where ω is the wave frequency, ℓ is the harmonic number, $\Omega_0 = eB_0/m_e c$ is the electron-cyclotron frequency using the rest mass, $\gamma = (1 - v_\parallel^2/c^2 - v_\perp^2/c^2)^{-1/2}$, $k_\parallel$ and $v_\parallel$ are the components of the wavenumber and particle velocity parallel to the magnetic field. For outside launch, these electrons can be trapped most easily by coherent ordinary modes near the electron-cyclotron frequency or extraordinary modes at the second harmonic for sufficient wave intensities if the electron trapping frequency ω_t is large enough so that $\omega_t \tau_c > 1$, where τ_c is the correlation time of the electron ($\tau_c \leq \tau_t = w/v_\parallel$ the transit time across the microwave beam along the field line) and if the collision frequency is less than the trapping frequency. In Ref. 2, an analysis of the relativistic Hamiltonian using canonical variables for an electron in a coherent ordinary or extraordinary wave is presented. At small wave amplitudes, the trapping frequency and the width of the trapped orbit in momentum space scale as $\alpha^{1/2}$ where $\alpha = (N_\perp/\sqrt{2})(v_\parallel/c)(\tilde{E}_\parallel/B_0)$ for an ordinary mode at the fundamental, $\alpha = (N_\perp/\sqrt{2})(\tilde{E}_\perp/B_0)$ for an extraordinary mode at the second harmonic, $N_\perp = k_\perp c/\omega$ is the perpendicular index of refraction and $\tilde{E}_\parallel$ and $\tilde{E}_\perp$ are the parallel and perpendicular components of the wave electric field. At larger amplitudes, the trapping width becomes comparable to the perpendicular momentum of the resonant electrons; one then enters a second nonlinear regime, where the trapping frequency and width scale as $\alpha^{1/(2-q)}$ where q $= 1/2$ for the ordinary mode at the fundamental and q $= 1$ for the extraordinary mode at the second harmonic.

In MTX, $\omega_t \tau_c \geq 10$ for thermal electrons and τ_c is much less than a collision time. Hence, most of the electrons are trapped; and this significantly alters the opacity of the plasma. If $\omega_t \tau_c < 1$, the resonant electrons would interact quasilinearly with the wave; and linear optical depths would be expected. Instead, most of the electrons in MTX transiting through the microwave pulse are trapped and interact adiabatically with the wave except when they enter the pulse and then exit. When they exit, they are

3

forced through an X point in phase space (see Fig. 1 of Ref. 2). Analysis and numerical studies with both a particle-orbit code and a self-consistent particle simulation confirm that trapping reduces the opacity in the case that $\nabla_\parallel k_\parallel = 0$ and $\nabla_\parallel B_0 = 0$, and the reduction is more severe with increasing wave amplitude.[2] In the first nonlinear regime, the nonlinear opacity scales as

$$\tau_{n\ell 1} \sim \tau_\ell p_2 / p_1^{1-q/2}, \tag{2}$$

where $\tau_\ell = \pi^2 (T_e/m_e c^2)\, (R/\lambda_0)\, (\omega_{pe}^2/\Omega_e^2)\, N$, $N = kc/\omega$, R is the magnetic-field scale length, λ_0 is the vacuum wavelength, $p_1 \equiv \alpha^{1/(2-q)}(m_e c^2/T_e)$, $p_2 \equiv (m_e c^2/T_e)\,(2\pi/\omega\tau_c)$, α is evaluated for a thermal electron, and $p_1 > p_2^{1/(1-q/2)}$ so that $\tau_{n\ell 1} < \tau_\ell$. In the second nonlinear regime, $p_1 > \max(1, p_2)$ and the nonlinear opacity is further reduced by the more extensive electron trapping,

$$\tau_{n\ell 2} \sim \tau_\ell p_2 / p_1^{2-2q}. \tag{3}$$

MTX parameters correspond to $p_1 \gtrsim 1$ and $p_2 < 1$, which puts the expected opacity in the second nonlinear regime. Figure 1 exhibits particle simulation results for O-mode absorption obtained from the ZOHAR relativistic, self-consistent, electromagnetic, particle simulation code.[3] The simulation results agree with the predictions of Eqs. (2) and (3) after correcting for the finite width of the plasma slab in the simulation, which was comparable to the width of the theoretical linear absorption layer and consequently narrower than the nonlinear absorption layers.

Toroidal effects and angular divergence of the microwave beam introduce parallel gradients in $k_\parallel$ and B_0, which can significantly improve the wave absorption over the predictions of Eqs. (2) and (3).[4] As a resonant electron transits the microwave pulse, it sees variations in both the cyclotron frequency and $k_\parallel$. This can result in an acceleration of trapped electrons as they follow the changing resonance condition, Eq. (1). This mechanism is the basis for rising-bucket current drive, which is discussed in Sec. III. The effect is illustrated in Fig. 2 where results for O-mode absorption obtained from a particle-orbit code are shown for cases with $k_\parallel = \nabla_\parallel B_0 = 0$ and $\nabla_\parallel B_0, \nabla_\parallel k_\parallel \neq 0$. In fact, by achieving a significant spread in $N_\parallel = k_\parallel c/\omega$, the parallel index of refraction, more electrons can be brought into resonance, their phases relative to the wave can be more readily decorrelated so as to limit the trapping, and the electrons can be better accelerated. The nonlinear optical depth $\tau_{n\ell}$ can thus be improved and even exceed the linear optical depth (Fig. 2b). Analytical and numerical calculations including parallel gradients have determined opacities for the Compact Ignition Tokamak (CIT) ($\tau_{n\ell} \gtrsim 5$) and for the single-pulse (3 GW, 30-50 ns) experiments in MTX during 1989 ($\tau_{n\ell} \sim 1$), which should be adequate for good absorption and heating.
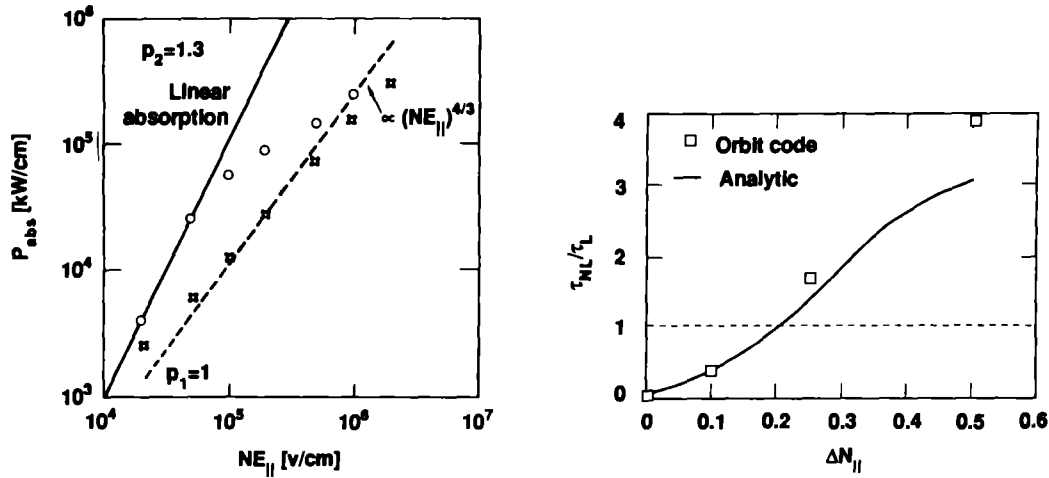
4

Figure 2: (a) Power absorbed for $k_\parallel = \nabla_\parallel B_0 = 0$ (crosses), and for $k_\parallel = 1.4 + 0.5(s - s_o)$ cm^{-1} with $\partial B_0/\partial s \neq 0$ corresponding to r = 3 cm in MTX (circles), $T_e = 1$ keV, $B_0 = 5$ T, $n_e = 1 \times 10^{14}$ cm^{-3}, and $p_2 = 1.3$. (b) Representative nonlinear opacities in MTX at 0.3 GW, 140 GHz, and $T_e = 1$ keV for O-mode heating.

III. Electron-Cyclotron Current Drive with Intense Microwaves

In addition to plasma heating, intense ECH can drive a toroidal current if waves with a particular sign of $k_\parallel$ are injected and if the single-pass absorption is sufficiently localized in space so that $\omega - \ell\Omega_o(\mathbf{x})/\gamma$ does not change sign and the current-carrying electrons share the same directionality along the field line. This follows from consideration of the resonance condition Eq. (1) and the role of the Doppler shift. If the resonant electrons are accelerated in either $v_\perp$, so that they are less collisional, or in $v_\parallel$, they will produce a toroidal current. Three new current-drive schemes that exploit FEL technology to achieve high efficiencies are described here: rising-bucket, stochastic, and beat-wave current-drive mechanisms.

A. Rising-Bucket Current Drive

The concept of rising-bucket current drive is analogous to acceleration in a synchrotron. One arranges for a spread in $k_\parallel$ or Ω_0 so that the resonance (1) shifts in energy as a function of position across the microwave beam. If the resonance shift is adiabatic as discussed in the following, a trapped electron remains trapped and so accelerates with the resonance. Gradients in $k_\parallel$ which lead to rising buckets can be produced by reflecting the incoming microwaves off a convex mirror placed in the mouth of the port (Fig. 3a).

The resonant electrons are accelerated from an initial resonance curve to a final
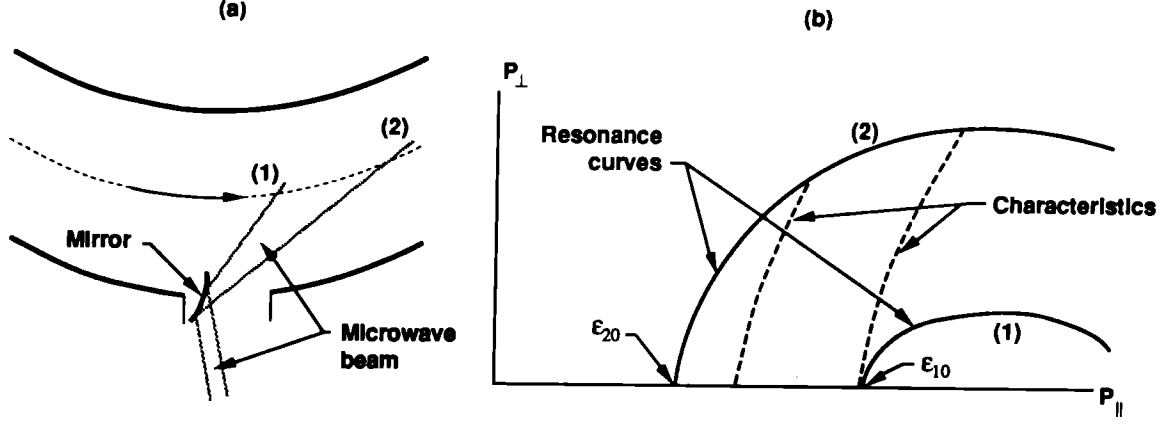
5

Figure 3: Rising bucket concept. (a) Microwaves launched into tokamak and reflected off convex mirror to spread $k_\parallel$. (b) Resonance curves and heating characteristics in momentum space.

one, both satisfying Eq. (1), along heating characteristics

$$\gamma m_e c^2 = \mu B_r + \text{const.} \tag{4}$$

where $B_r \equiv m_e c\omega/e$ and μ is the relativistic magnetic moment (Fig. 3b). The energy gain for the typical situation in which magnetic gradients are insignificant across the beam is given by:

$$\Delta \gamma m_e c^2 = p_{\parallel i} c \left[-N_{\parallel i} + N_{\parallel f} \left(\frac{1 - N_{\parallel i}^2}{1 - N_{\parallel f}^2} \right)^{1/2} \right], \tag{5}$$

where $N_{\parallel i}$ and $N_{\parallel f}$ are the initial and final parallel indices of refraction and $p_{\parallel i}$ is the initial parallel momentum. Rising buckets are most effective at improving the local current-drive efficiency when $N_{\parallel f}$ is near one. This requires the microwaves to be nearly tangent to the resonant flux surface and $N \lesssim 1$, so that $\omega_{pe}^2 \ll (\ell\Omega_0)^2$ or $\ell \geq 3$ for an extraordinary wave and $\ell \geq 2$ for an ordinary wave. The ray paths for the microwaves will be nearly straight. For smaller $N_{\parallel f}$, rising buckets can improve the ray-path-integrated efficiencies by increasing the opacity for a sufficiently large spread in $N_\parallel$; the product of the energy gain and number of resonant electrons can exceed that for the case with no trapping, i.e., the quasilinear limit; and $\tau_{n\ell} \geq \tau_\ell$ can be achieved (Fig. 2b).

In order for the resonant electrons to remain trapped in a rising bucket, the bucket must be lifted adiabatically; that is, the wave electric field must be able to accelerate electrons fast enough to keep up with the accelerating resonance. This implies a lower-bound constraint on the intensity of the applied microwaves. The dependence of this constraint on the cyclotron harmonic number introduces harmonic selectivity which

6

can help overcome unwanted competition from neighboring harmonic resonances.[5] A preliminary analysis of a rising-bucket current-drive scenario for ITER using a third-harmonic extraordinary mode indicates high opacity ($\tau_{n\ell} > 100$), harmonic selectivity ($\ell = 4$ is nonadiabatic and $\tau \sim 1$), and good current-drive efficiencies $\eta \equiv nIR/P = 0.3 - 0.6 \times 10^{20}$ A/m^{2}W on sample flux surfaces (compared to $\eta \approx 0.3 \times 10^{20}$ A/m^{2}W for quasilinear ECH on the best flux surface).

B. Stochastic Current Drive

Another current-drive scheme exploiting high intensity is stochastic current drive due to overlap of cyclotron harmonic resonances.[6] This nonlinear phenomenon occurs when the nonlinear island (or trapping) width exceeds the separation between neighboring islands. The stochastic electrons then diffuse along characteristics given by

$$\mathcal{E} - \omega p_{\|}/k_{\|} = \text{const.} \tag{6}$$

where $\mathcal{E}$ is the particle energy. By choosing waves with a particular sign of $k_{\|}$, e.g., $k_{\|} > 0$, electrons with $p_{\|} > 0$ can be diffused to higher energies and concomitanty larger values of $p_{\|}$. Both their reduced collisionality at higher energies and their increased $p_{\|}$ combine to give a current.

Numerical studies of the particle orbits indicate that the best conditions for stochastic current drive are obtained from extraordinary modes with $\omega/\Omega_0 = 1.8 - 1.9$, and $\bar{E}/B_0 \geq 0.1$ is required to induce stochasticity and achieve good current-drive efficiencies. Such a large electric field intensity significantly exceeds those expected in MTX and would require focusing the microwave down with a concave mirror. The use of ordinary modes near the cyclotron frequency requires even higher field strengths $\bar{E}/B_0 \geq 0.3$. The current-drive efficiencies achieved with extraordinary waves are high ($\eta \geq 0.15 \times 10^{20}$ A/m^{2}W) and only very weakly dependent on plasma temperature because the heated electrons acquire energies so much higher than the bulk plasma temperature (Fig. 4).

C. Beat-Wave Current Drive

Beat-wave current drive[7] involves beating two intense microwave beams to resonantly excite a longitudinal wave, e.g., a Langmuir wave propagating along the magnetic field or an obliquely propagating upper-hybrid wave. So far we have considered Langmuir waves resonantly driven by the beating of two cyclotron waves.[7] The Langmuir waves Landau damp on electrons leading to a current. This scheme is an example of a resonant three-wave interaction with frequency and wavenumber matching conditions: $\omega_1 - \omega_2 = \omega_3$, $\mathbf{k_1} - \mathbf{k_2} = \mathbf{k_3}$. There are a number of requirements to be met for
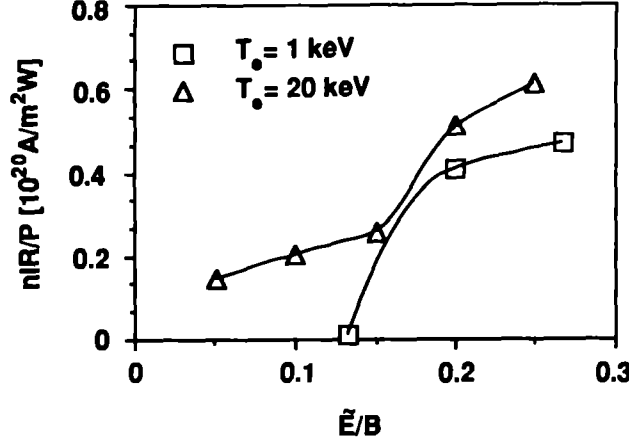
Figure 4: Current-drive efficiency $\eta = \text{nIR}/\text{P}$ ($10^{20}\text{A}/\text{m}^2\text{W}$) as a function of relative electric field strength $\tilde{E}/B_0$ for stochastic current drive.

the achievement of high efficiency in beat-wave current drive. The difference frequency of the two microwave beams must match the electron plasma frequency where the current is to be excited. The difference wavenumber must have a substantial component along the field line, and the beat-wave phase velocity must not fall too far out on the tail of the electron distribution function so that there are insufficient electrons to damp the Langmuir wave and carry all the current. The two transverse waves should be similarly polarized. Finally, the product of the two microwave beam powers must exceed a threshold condition in order to deposit much momentum in the plasma.[7]

A nonlinear wave equation is derived in Ref. 7 that describes the conservation of wave action flux at steady state and from which the ultimate efficiency of beat-wave current drive can be deduced:

$$\hat{k}_1 \cdot \nabla J_1 = -\frac{2\pi k_3^2}{k_1 k_2} J_1 J_2 \text{Im}[\chi_e(1 + \chi_i)/\epsilon] = -\hat{k}_2 \cdot \nabla J_2 \qquad (7)$$

where $J_{1,2} = (k_{1,2}/2\pi) \mid \underline{u}_{1,2}/c \mid^2$ are the transverse-wave action flux densities in natural units, $\underline{u}_{1,2}$ are the electron quiver velocities in the waves, χ_e and χ_i are the linear electron and ion suceptibilities, and $\epsilon = 1 + \chi_e + \chi_i$. The wave energy flux densities or the power densities are given by $\omega_{1,2}J_{1,2}$. Conservation of wave action for collinear wave propagation asserts that $\Delta J_1 = \mp \Delta J_2$ for parallel/anti-parallel wave orientations. Relative to the energy originally available in the two transverse waves, only a fraction $q_e = \omega_3/[\omega_1(1 + \omega_2\rho/\omega_1)]$ can be acquired by the beat wave as a consequence of action conservation ($\rho = J_2^{in}/J_1^{in}$ is the input ratio of action fluxes). Furthermore, analytical calculations determine that the pump-depletion factor $R_a \equiv \Delta J_1/J_1^{in} \rightarrow 1$ for $(\pi k_3^2 L/k_2)(u_1 u_2/c^2) > 1$. Where $L^{-1} \equiv \mid \nabla \ln n_e \mid$. The beat-wave current-drive efficiency
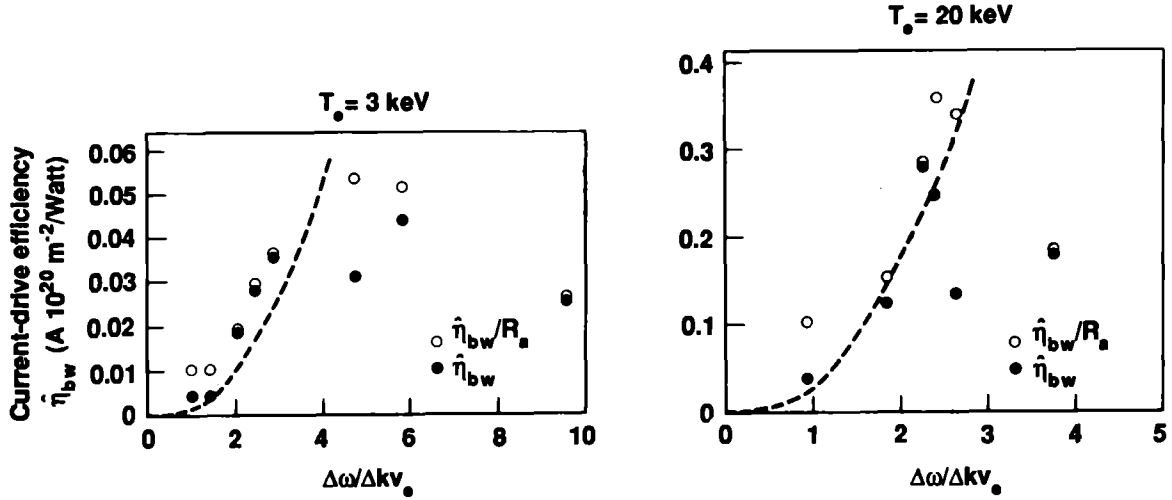
8

Figure 5: Beat-wave current-drive efficiency $\hat{\eta}_{bw}$ and $\hat{\eta}_{bw}/R_a$ (to correct for incomplete action transfer in artifically short simulations) as a function of beat-wave relative phase velocity $\Delta\omega/\Delta kv_e$ for MTX and reactor cases.

η_{bw} accounting for collisional relaxation of the electrons is related to the efficiency for a Landau-damped plasma wave by the relation

$$\eta_{bw} = nIR/P_{pumps} = \eta_{LD}q_e R_a, \tag{8}$$

where η_{LD} is the lower-hybrid-like current-drive efficiency for a Landau-damped wave.[8] The validity of Eq. (7) depends on the beat wave being completely Landau damped by the electrons. Particle simulations with a one-dimensional, relativistic, self-consistent electromagnetic particle code have determined that the electrons fully damp the beat-wave, pump depletion is nearly complete, and coupling to the ions is weak for beat wave phase velocities ω_3/k_3 satsifying $1.5 < \omega_3/k_3v_e < 4$ where $v_e = (T_e/m_e)^{1/2}$ (Fig. 5).

Beat-wave current-drive offers the opportunity for high efficiencies and precise control over where and when the current is driven. Unwanted competition from neighboring cyclotron harmonics is easily avoided, and degradation of the current drive by trapped-particle effects is weak. The accessibility of the beat wave is readily guaranteed by the accessibility of the two driving waves. The price of this is the use of two intense microwave sources and the reduction of the current-drive efficiency by the factor $q_e R_a$ in Eq. (7), where $q_e \lesssim 1/3$ in most practical applications. The current-drive efficiency for Langmuir beat waves increases linearly with temperature and approaches 0.4×10^{20} A/m^{2}W for a 20 keV plasma (Fig. 5). The use of a cyclotron-auto-resonant upper-hybrid beat wave might lead to higher current-drive efficiencies that are less dependent on the plasma bulk temperature.[7]

9

IV. Intense Lower-Hybrid Current Drive

Lower-hybrid current drive with conventional microwave sources has previously been regarded as unsuitable for use in the core of a reactor plasma because the requirement of accessibility restricts the wave phase velocity to be so low that electron Landau damping is severe. However, the electron distribution cannot absorb any more power than that required to form a plateau in the range of velocities resonant with the wave phase velocity. Hence, the invention of intense, pulsed microwave sources in the 10 GHz frequency range, e.g., relativistic klystrons,[9] provides the possibility of improved lower-hybrid wave penetration in a reactor using sources with high peak but moderate average power. This scheme is appealing inasmuch as lower-hybrid current drive and heating have a strong experimental data base, the theoretical current-drive efficiencies are high (comparable to the rising-bucket scheme described here), and the deformation of the electron distribution function resulting from the intense lower-hybrid waves is relatively modest and more likely to be microstable.

Calculations have been made to estimate the power required to penetrate the plasma a given distance by forming a plateau in velocity space with pulsed microwaves. In the limit that the plateau relaxes between successive pulses, the *peak* power is independent of the repetition rate and is that needed to form the plateau from an initially Maxwellian plasma. The penetration distance scales explicity as the power and inversely as the product of the cube of the relative plateau width (which also depends on power) in parallel velocity and the number of electrons per unit area. In the limit that the pulse repetition rate is so rapid that there is no relaxation of the electron distribution function in between pulses, the *average* power required to penetrate a given distance is independent of the repetition rate and is the same as that for continuously applied power which is that necessary to balance collisions; and the penetration distance scales inversely as the relative velocity width of the plateau.

In general, for fixed average (peak) power and pulse length, the penetration distance is increased by decreasing (increasing) the repetition rate. The plateau width is determined by the spread in the $N_\parallel$ spectrum and single-pass acceleration (including nonlinear orbit effects). For representative ITER parameters ($n = 0.6 \times 10^{20}$ m^{-3}, $T_e = 25$ keV, and B = 5.1 T) and $N_\parallel$ at the accessibility limit, the penetration distance is 1.6 m at the minimum plateau width $\Delta v_\parallel / v_\parallel \approx 0.13$ for infrequent 10 GHz, 10 GW pulses compared to about 18 cm for linear Landau damping. The average power is independently set by the pulse repetition rate. The overall scaling with peak power is weak. In the frequent-pulse limit, the same penetration is achieved with an average power of 210 MW. The important point here is that the average power for the case of high peak-power, infrequent pulses can be made much smaller than that in the

frequent-pulse or continuous limit to achieve the same penetration.

V. Complications Associated with Intense Microwaves

The high intensities of the microwaves used in the applications described here and the significant acceleration and heating of the electron distribution function produced can lead to certain unwanted complications. The intense microwave fields can excite parametric instabilities,[10] for example, stimulated backscattering and side scattering that can prevent all of the microwave beam from reaching the resonance layer or anomalous absorption via parametric decay into longitudinal modes that can alter the heating profile. The nonlinear ponderomotive force of the microwave beam can lead to self-focusing of the microwaves and a concomitant local depletion of the plasma density.[11] Strong local heating of the electron distribution can generate significant local perturbations in the electrostatic potential that can influence particle drifts and transport.[12] The nonlinear trapping of electrons in the intense microwaves can destabilize forward scattered sidebands of the principal wave; however, this instability has been found to be very weak for MTX parameters.[13] Finally, the strong heating of the electron velocity distribution can lead to microinstability and anomalous transport. We assess the importance of these phenomena because of the threat they pose to the success of the intended applications. In this section we give examples of some of these complications.

A. Parametric Instabilities for Intense ECH

Parametric instabilities for intense ECH have received attention in Ref. 10, where a survey of instabilities for perpendicularly incident ordinary modes at the cyclotron frequency and extraordinary modes at the second harmonic was presented. A schematic of some of the principal instabilities is reprised in Fig. 6. For ordinary-mode heating in MTX, the most worrisome instability is Brillouin backscatter by electrostatic ion-cyclotron waves and ion quasi-modes. In the initial experiments in 1989 at $\lesssim 3$ GW and with 30 ns pulses in a deuterium plasma and frequency 140 GHz, the power levels exceed thresholds for Brillouin backscatter; but the short pulse length limits the growth of the instability to less than five or six e-foldings. Subsequent experiments planned at 250 GHz and 50 ns may be subject to significant Brillouin backscatter. The following analytical arguments and results from a one-dimensional electromagnetic particle simulation illustrate some of the physics of Brillouin backscatter in a magnetized plasma and serve as a useful paridigm.

Consider the backscatter of a perpendicularly incident ordinary wave ($\mathbf{k_0} \cdot \mathbf{B_0} = 0$) by a perpendicularly propagating lower hybrid wave. The calculation of the frequency and growth rate has been given in Ref. 14. The steady-state coupled-mode equations
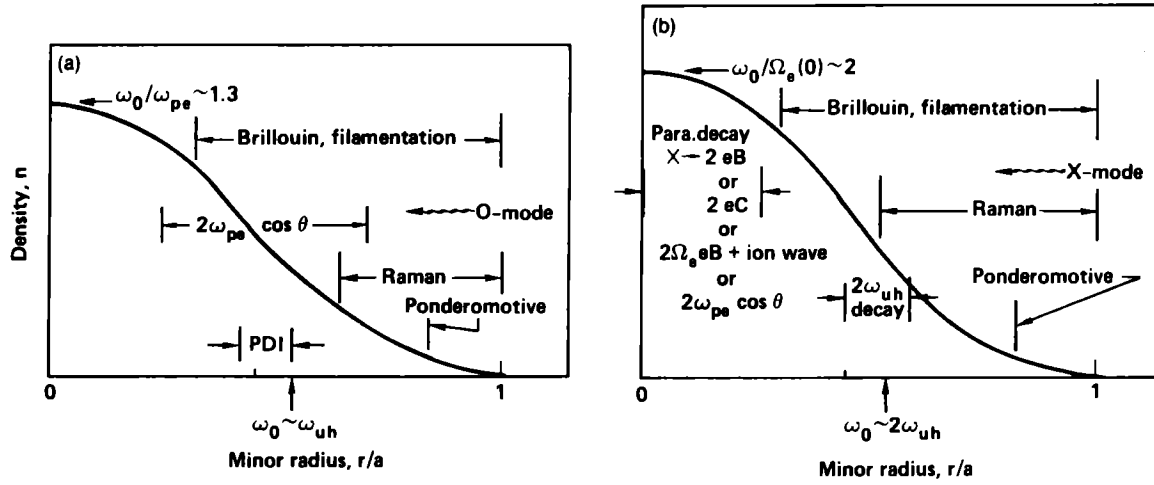
Figure 6: Schematic of parametric processes associated with (a) ordinary ($\omega_0 \approx \Omega_e$) and (b) extraordinary ($\omega_0 \approx 2\Omega_e$) wave heating. eB denotes electron Bernstein wave, eC denotes electron cyclotron, and PDI is parametric decay instability.

for the pump wave and the backscattered radiation are readily deduced from Maxwell's equations and a simple fluid theory,[15]

$$\frac{\partial}{\partial x}a_0 = -\alpha\frac{\delta n_e}{n_0}a_1 \tag{9}$$
$$\frac{\partial}{\partial x}a_1 = -\alpha\frac{\delta n_e}{n_0}a_0,$$

where δn_e is the perturbed electron density in the ion wave, $a_{0,1}$ are the vector potentials for negligibly damped transverse modes, $\alpha \equiv (\pi/2)(\omega_{pe}^2/\omega_0^2)\lambda_0^{-1}(1-\omega_{pe}^2/\omega_0^2)^{-1/2}$, and λ_0 is the vacuum wavelength of the pump wave. For backscattering over a uniform plasma of length L, Eq. (8) is readily integrated for constant $\alpha\delta n_e/n_o$ to obtain a reflection coefficient for Brillouin backscatter

$$R_b = \mid a_1(0)/a_0(0) \mid^2 = \tanh^2(\alpha L\delta n_e/n_0). \tag{10}$$

The reflection coefficient at saturation is then set by the amplitude of the ion wave.

On a relatively short time scale determined by the growth rate of the instability, the ion wave can grow up and trap ions before significant heating or deformation of the equilibrium density profile can occur. Because of the strong background magnetic field across which plasma must be transported in order to steepen the density profile, profile steepening as a possible saturation mechanism is inhibited. Because the frequency of the lower hybrid wave $\omega_{lh} = \omega_{pi}/(1 + \omega_{pe}^2/\Omega_e^2)^{1/2}$ greatly exceeds the ion-cyclotron frequency, an unmagnetized description of the ions suffices to describe their trapping. From a simple waterbag model,[16] an approximate trapping criterion can be derived:

$$\frac{e\delta\phi}{m_i} \geq \frac{1}{2}\left(\frac{\omega_{lh}}{k} - \sqrt{3}v_i\right)^2 \rightarrow \frac{\delta n_e}{n_o} \geq \frac{1}{2}\frac{m_i}{m_e}\frac{\omega_{lh}^2}{\Omega_e^2}\left(1 - \sqrt{3}\frac{kv_i}{\omega_{lh}}\right)^2 \tag{11}$$
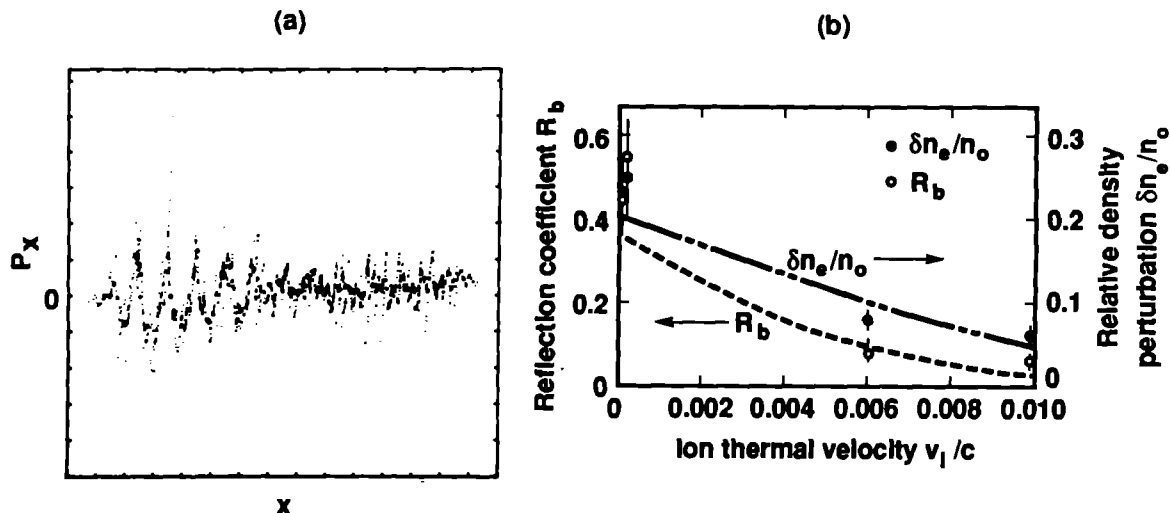
12

Figure 7: (a) Ion phase space, momentum p_x vs. x, showing the onset of ion trapping. (b) Perturbed electron density $\delta n_e/n_o$ and reflection coefficient for Brillouin backscatter $R_b = |a_1(0)/a_0(0)|^2$ at saturation as functions of relative ion thermal velocity.

where $\delta\phi$ is the electrostatic potential perturbation, $\Omega_e = eB_0/m_e c$, $k \approx 2k_0$, $v_i = (T_i/m_i)^{1/2}$, and the electron response is assumed to be linear. Use of Eq. (10) for $\delta n_e/n_0$ in Eq. (9) relates the reflection coefficient to the ion temperature. Figure 9a shows the significant ion trapping in a snapshot of the ion phase space from a ZOHAR particle simulation, while in Fig. 7b, we plot simulation results for the relative density perturbation and reflection coefficient at saturation compared to the theoretical estimate of Eqs. (9) and (10) as a function of the ion thermal velocity. Fairly good agreement with theory is obtained, and we note the strong effect that increasing the ion temperature has on reducing the reflection coefficient. The analysis for backscatter by electrostatic ion-cyclotron waves is similar but differs inasmuch as the ions are magnetized, which alters the trapping criterion.[17]

B.   Nonlinear Self-Focusing

The strong ponderomotive force on the electrons in the intense microwaves can lead to a local depletion of the electron density that focuses the radiation and further enhances the ponderomotive force and the density depletion. In Ref. 10, the convective growth of a small-amplitude filament in a microwave beam of infinite lateral extent was calculated. For MTX parameters, the linear growth length of the fastest growing mode is comparable to the minor radius so that the growth of a filament from a very small-amplitude hot spot is not significant. However, the pinching of an intense microwave beam with a finite lateral extent evolves quite differently, and nonlinear whole-beam self-focusing in MTX could be significant.[11]

13

Consider the nonlinear wave equation describing electromagnetic wave propagation in a plasma[10,11,18]

$$\frac{\partial^2}{\partial t^2}\mathbf{E} + \nabla(\nabla \cdot \mathbf{E}) - \nabla^2\mathbf{E} + \frac{4\pi}{c^2}\frac{\partial}{\partial t}\mathbf{J} = 0, \tag{12}$$

where a fluid model for the electron response in an ordinary wave that is incident perpendicular to the background magnetic field $\mathbf{B_0}$ or for ($\mathbf{B_0} = 0$) gives $\partial \mathbf{J}/\partial t = ne^2\mathbf{E}/m_e$. For finite $k_\parallel v_e$ and $k_\parallel v_i$, the quasi-steady magnetized plasma response to the ponderomotive force produced by the high-frequency electromagnetic waves is[18]

$$n = n_o exp\left[-e^2\left\langle E^2\right\rangle /2m_e\omega_0(T_e + T_i)\right] \tag{13}$$

(Reference 11 has examined the effects of ion inertia on the dynamical evolution of self-focusing.) An over-estimate of the self-focusing is given by a steady-state solution of Eqs. (12) and (13) in the paraxial limit.[18] Use of the saturable, exponential nonlinearity in Eq. (13) precludes catastrophic focusing to a point. Relaxing the paraxial approximation by retaining second derivatives along the microwave beam would also prevent catastrophic self-focusing.

If a Gaussian ansatz for the beam profile is adopted as in Ref. 18, solutions for the relative beam radius as a function of the propagation distance into the plasma can be obtained by integrating a one-dimensional differential equation deduced from Eq. (12) with the angular divergence or convergence of the microwave beam at incidence as the boundary condition. Representative solutions for the relative beam radius are exhibited in Fig. 8 for MTX parameters. Increasing the angular divergence of the incident microwave beam pushes the focus farther downstream. The focus also occurs farther downstream for Gaussian density and temperature profiles than it does for square profiles. Cyclotron absorption at the resonance layer ($z \approx 15$ cm in Fig. 8) has not been included in this calculation. From these estimates we conclude that there could be appreciable, but tolerable self-focusing in MTX, which can be lessened by spreading the beam over a larger spot size to reduce the field strength or by increasing the angular divergence of the beam at incidence. Such remedies for self-focusing should be even more easily arranged in future, larger experiments.

C. Microinstability of Strongly Heated Electron Distributions

Acceleration and heating of the electrons with intense microwaves can lead to significant deformations of the velocity distribution function. The results of a numerical evaluation of ordinary-mode heating at the fundamental for representative MTX parameters using a non-self-consistent particle-orbit code are shown in Fig. 9. Because collisional relaxation of the heated distribution function occurs on a time scale that is
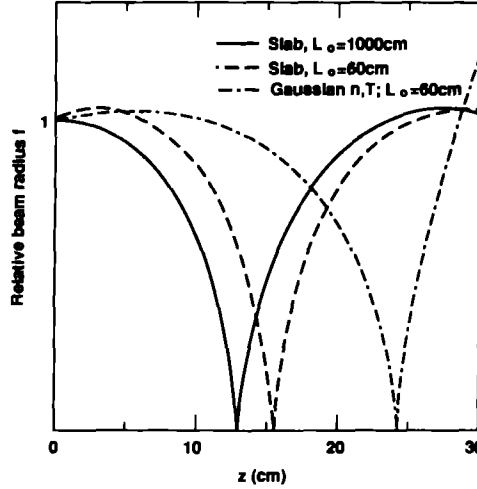
14

Figure 8: Relative microwave beam radius f as a function of penetration distance into the plasma for MTX parameters with $L_0^{-1} \equiv d\ln f/dz$ at $z = 0$, $v_0^2/4v_e^2(1 + T_i/T_e) = 0.03$, $T_i = T_e = 1$ keV, and $\omega_{pe}^2/\omega_0^2 = 0.5$ on axis in the core of the plasma.

much longer than the pulse of the FEL and there is both a significant energy inversion and anisotropy, we expect that high-frequency electron microinstabilities may be excited, e.g., whistlers, upper-hybrid loss-cone, and cyclotron maser instabilities. This has been studied in the context of strong ECH in tandem mirrors.[19] The microturbulence is expected to diffuse the electron velocity distribution function and relax the free-energy driving the instability. Work in progress with the ZOHAR two-dimensional particle simulation code modeling intense ECH suggests that the electron distribution function can relax in this manner. Detailed calculations of electron microinstability and its influence on electron energy confinement await future analysis.

D.   Parametric Instability for Intense Lower-Hybrid Waves

Parametric instabilities are an important issue for intense lower-hybrid waves. For the wave fields under consideration in Sec. 4, $N_\perp E_\perp/B_0 \lesssim 1$, so that the conventional perturbation theory of weak parametric instabilities may not be valid. Therefore, the code described in Ref. 20 has been used to determine growth rates for parametric decay into a low-frequency quasi-mode and a sideband lower-hybrid wave with maximum growth rates varying from $1 \times 10^8 s^{-1}$ to 2×10^9 s^{-1} as the peak power is varied from 1 to 100 GW/m^2 for plasma parameters characteristic of the edge of ITER, $n_e \approx (1 - 5) \times 10^{19}$ m^{-3} and $T_e \approx (0.1 - 0.8)$ keV. The convective instability threshold for a 1 m wide grill is of the order of $\gamma_o \approx 1 \times 10^8$ s^{-1}, corresponding to $P \approx 1$ - 2 GW/m^2. For pulses of length 20-50 ns, these results suggest that the peak power be kept down to a few GW/m^2, implying from the discussion of Sec. IV that, for good penetration,
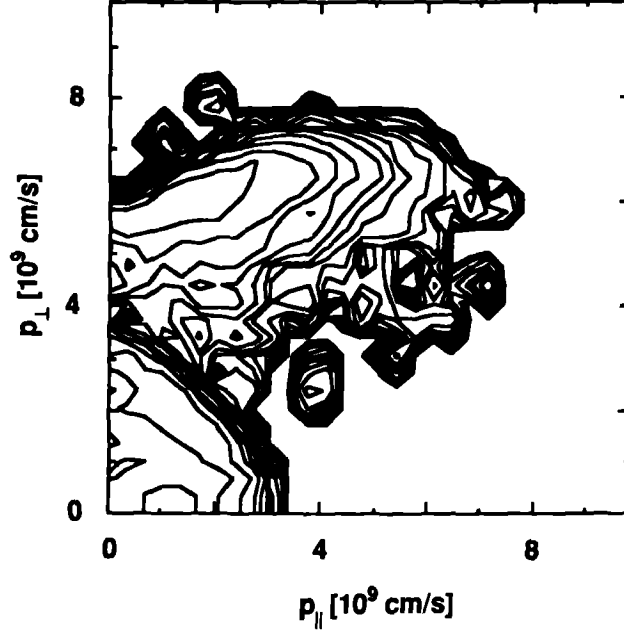
15

Figure 9: Contour plot of electron distribution function in momentum space after single-pulse, FEL heating by an O-mode with $\tilde{E}_{rf} = 5 \times 10^5$ V/cm.

the spectrum must be kept narrow, $\Delta N_{\parallel}/N_{\parallel} \leq 10\%$. The latter requirement is being explored with a ray-tracing code, and preliminary results are encouraging.

VI. Discussion

In this paper we have described the application of intense, pulsed microwaves to heat plasma and drive current. The new microwave sources possess certain inherent technological advantages, e.g. tunability, high power, and ease of transmission, and lead to technical advantages in their applications: improved efficiency, improved access to the core plasma, and precise control of the deposition profile. The absorption of the intense waves can be nonlinearly improved over the quasilinear absorption (Fig. 2b). In addition, the use of intense ECH and lower-hybrid waves can lead to current-drive efficiencies that are better than those obtained by the lower-peak-power, quasi-linear mechanism (Table 1). The current-drive efficiencies cited throughout this paper are calculated as in Ref. 21, and include both trapped-particle and relativistic effects, but exclude momentum-conserving corrections to the collision operator and part of the energy diffusion contributed by background electrons.[22] These excluded effects can improve the current-drive efficiency by an additional factor of relative order T_e/ϵ_r, where ϵ_r is the energy of a typical resonant electron.

There are several other benefits associated with the use of these new microwave

16

Table 1: Representative current-drive efficiencies nIR/P [10^{20} A/m²W].

	MTX	CIT	ITER
Quasilinear	0.03-0.04	0.1 - 0.15	0.2 - 0.3
Beat waves	0.03- 0.05	0.2	0.2 - 0.4
Rising buckets	0.05 - 0.1	0.2 - 0.4	0.3 - 0.6
Stochastic	0.1 - 0.2	0.15 - 0.3	0.2 - 0.4

sources. Because of the tunability of these sources and the resonant nature of the interaction of the waves with the plasma, the plasma heating and current-drive schemes described here afford the opportunity for shaping the pressure and current profiles in the plasma with some precision. This leads to the possibilities of controlling sawteeth oscillations by modifying the current profile and preventing disruptions by driving current at magnetic islands with a phase opposite to that of the tearing mode. A frequency-tunable source would also be advantageous for heating and current drive during the ramping up of the toroidal magnetic field, as well as during the flat-top phase.

Many of the important physics issues associated with the application of intense microwave sources to heating and current drive have been addressed only in a preliminary fashion so far. Furthermore, the examples given in Sec. 5 indicate that some possibly important complications may arise in using intense sources. Nevertheless, our calculations make it clear that there are many exciting new opportunities to better heat and drive current in tokamaks.

The MTX experiment will provide an important testbed for exploring the physics of nonlinear absorption, rising buckets, stochastic acceleration, and possibly intense lower-hybrid-wave heating, as well as providing some experimental assessment of the importance of parametric instabilities, nonlinear self-focusing, and microinstabilities. It is important to keep in mind that some of the more worrisome complications, viz., parametric instabilities and nonlinear self-focusing, will be much less threatening in applications to larger experiments where expanded port areas will allow the electric field intensities to be reduced. Thus, there are many reasons to be optimistic about the future use of intense microwave sources to improve the efficiency of both heating and driving current in tokamaks.

Acknowledgement

References

[1] K.I. Thomassen, ed *Free-Electron-Laser Experiments in Alcator-C* (U.S. Government Printing Office, Washington, D.C., 1986).

[2] W.M. Nevins, T.D. Rognlien, and B.I. Cohen, Phys. Rev. Lett. **59** 60 (1987).

[3] A.B. Langdon and B.F. Lasinski, Method Comput. Phys. **16**, 327 (1976).

[4] R.H. Cohen, B.I. Cohen, W.M. Nevins, T.D. Rognlien, P.T. Bonoli, and M. Porkolab, "Current Drive by Intense Microwave Pulses," in *Nonlinear Phenomena in Vlasov Plasmas* (Proc. of the Cargese Workshop, 1988), Lawrence Livermore National Laboratory Report UCRL-99583 (September, 1988).

[5] G.R. Smith, R.H. Cohen, and T.K. Mau, Phys. Fluids **30**, 3633 (1987).

[6] C.R. Menyuk, A.T. Drobot, K. Papadopoulous, and H. Karimabadi, Phys. Rev. Lett. **58**, 2071 (1987).

[7] B.I. Cohen, Comments Plasma Phys. Cont. Fusion **8**, 197 (1984); B.I. Cohen, R.H. Cohen, B.G. Logan, W.M. Nevins, G.R. Smith, A.V. Kluge, and A.H. Kritz, to appear in Nucl. Fusion, 1988.

[8] N.J. Fisch, Rev. Mod. Phys. **59**, 175 (1987).

[9] A.M. Sessler, Physics Today **41**, No. 1, 26 (1988).

[10] M. Porkolab and B.I. Cohen, Nucl. Fusion **28**, 239 (1988).

[11] A. Cardinali, M. Lontano, and A.M. Sergeev, in *Proceedings of the 15th European Conference on Controlled Fusion* (Ed. S. Pesic, J. Jacquist), Dubrovnik, Yugoslavia, May 16-20, 1988 (Europhysics Confs. Abs., 1988), Vol. 12 B, Part III, p. 976.

[12] A.J. Lichtenberg, M.A. Lieberman, and R.H. Cohen, Physi. Fluids **30**, 3540 (1987).

[13] B.I. Cohen and R.H. Cohen, Phys. Fluids, to appear (1988).

[14] B.I. Cohen, Phys. Fluids **9**, 2676 (1987).

[15] W.L. Kruer, Phys. Fluids **23**, 1274 (1980).

[16] J.M. Dawson, W.L. Kruer, and B. Rosen, in *Dynamics of Ionized Gases*, ed. M. Lighthill, I. Ionai, and H. Sato (Univ. of Tokyo Press, Tokyo, 1973), p. 47.

[17] B.I. Cohen, N. Maron, and G.R. Smith, Phys. Fluids **25**, 821 (1982).

[18]C.E. Max, Phys. Fluids **19**, 74 (1976).

[19]Y.J. Chen, W.M. Nevins and G.R. Smith in *Hot Electron Ring Physics* (Proc. 2nd Workshop, San Diego, 1981), Vol. I, CONF-811203, Oak Ridge National Laboratory, Oak Ridge, TN (1982), p. 279.

[20]M. Porkolab, Phys. Fluids **20**, 2058 (1977).

[21]R.H. Cohen, Phys. Fluids **30**, 2442 (1987) and erratum in Phys. Fluids **31**, 421 (1988).

[22]C.F.F. Karney and N.J. Fisch, Phys. Fluids **28**, 116 (1985).